

Hyperspherical partial wave calculation for double photoionization of the helium atom at 20 eV excess energy

J. N. Das[†], K. Chakrabarti[‡] and S. Paul[†]

[†] Department of Applied Mathematics, University College of Science, 92 Acharya Prafulla Chandra Road, Calcutta - 700 009, India

[‡] Department of Mathematics, Scottish Church College, 1 & 3 Urquhart Square, Calcutta - 700 006, India

E-mail: jndas@cucc.ernet.in

Abstract. Hyperspherical partial wave approach has been applied here in the study of double photoionization of the helium atom for equal energy sharing geometry at 20 eV excess energy. Calculations have been done both in length and velocity gauges and are found to agree with each other, with the CCC results and with experiments and exhibit some advantages of the corresponding three particle wave function over other wave functions in use.

Submitted to: *JPB*

1. Introduction

There has been a significant development in the last one decade in the theoretical study of double photoionization (DPI) of the helium atom. This was possible because of rapid developments in the experimental side by several groups, extending over several countries. Double photoionization of the helium atom is one of the most basic atomic processes. Even then, this problem merits further detailed studies as it involves complex three body effects and electron correlations that are not yet fully understood. Total DPI cross section for helium has been measured by several groups [1, 2, 3, 4] and also calculated theoretically by many others [5, 6, 7, 8]. In general there is good agreement between the observed and the calculated cross sections. However, there are also some discrepancies. For example experimental results of Samson *et al* and of Bizau and Wulleumier, although agree within 15 percent of each other, there are systematic differences at energies above 1 Rydberg. So also is the case regarding the theories. Results of hyperspherical \mathcal{R} -matrix with semi-classical outgoing waves (HRM-SOW) of Selles *et al* [9] agree favourably with the results of Bizau and Wulleumier [1] while the 2SC calculation of Pont and Shakeshaft [5] favours the measurements of Samson *et al* [4] (see ref. [9]). As regards the differential cross-sections, understanding of the results

has much improved with the availability of results of some elaborate calculations like the time-dependent close coupling (TDCC) calculation of Colgan *et al* [7], the HRM-SOW calculation of Malegat *et al* and Selles *et al* [8, 9] in addition to the earlier results ([10, 11, 12, 13]) and the recent results ([14, 15, 16] of CCC theory, the most extensively applied theory to the problem to date. For the status of the CCC and some other methods the review article by Briggs and Schimdt [17] may be seen. Even then there remains the task of improving the theoretical estimates, particularly at low energies and for unequal-energy-sharing geometries (for which the results appear comparatively less satisfactory) as well as for better understanding of the physics of the DPI problem of helium

In the time-independent frame work the solution of the problem depends basically on the accurate computation of the T-matrix element given by

$$T_{fi} = \langle \Psi_f^{(-)} | V | \Phi_i \rangle, \quad (1)$$

where $\Phi_i(\vec{r}_1, \vec{r}_2)$ is the helium ground state wave function, V is the interaction term given by

$$V = \vec{\epsilon} \cdot \vec{D}. \quad (2)$$

\vec{D} is the dipole operator and is given $\vec{D} = \vec{\nabla}_1 + \vec{\nabla}_2$ (velocity form) or $\omega_i(\vec{r}_1 + \vec{r}_2)$ (length form) and $\Psi_f^{(-)}(\vec{r}_1, \vec{r}_2)$ is the final channel continuum wave function with incoming wave boundary condition for the two outgoing electrons and ω_i is the incident photon energy. Here $\vec{\epsilon}$ is the photon polarization direction and \vec{r}_1, \vec{r}_2 are the co-ordinates of the two outgoing electrons, the nucleus being at the origin.

For accurate cross section results one needs accurate wave functions Φ_i and $\Psi_f^{(-)}$. Accurate bound state helium wave functions are easily available. There exists a number of such wave functions for the ground state (and low-lying excited states) in analytic form of different accuracies, such as simple Hartree Fock type wave function used by Maulbetsch and Briggs [18] or a Hylleraas type wave function given by Chandrashekar and Herzberg [19] or by Hart and Herzberg [20]. If needed, one may also readily generate an arbitrarily accurate bound state wave function along the line developed by Pekeris [21]. But for $\Psi_f^{(-)}$ there are no such simple accurate wavefunctions in analytical form. Most wave functions used in the literature are either incorrect at finite distances or in the asymptotic domain, as 3C [22] or 2SC [23] wave functions. There are now many calculations of varied accuracies depending mainly on the use of different final channel wave functions.

Without caring for the explicit form of the wave functions, Huetz and co-workers [24] established dependence of cross sections on various angular variables of the outgoing electrons and on energy. For the equal energy sharing geometry case it turns out to be rather simple in form. On least squares fitting this gives good representation of the triple differential cross section(TDCS) results (some authors prefer the name five fold differential cross sections (FDSC) which is more appropriate and relevant in view of some recent experimental results [25]. However, we will continue to call it TDCS).

For the study of TDCS close to threshold there are the Wannier calculations by Faegin [26, 27]. These give good representation of the shape of TDCS results at 6 eV excess energy but miserably fail at higher energies.

There are also a number of detailed calculations by Maulbetsch and Briggs [18, 28] which used for the final state wave function, the 3C wave function of BBK theory [22] and produced moderately accurate cross section results. It is well known that the 3C wave function is correct in the asymptotic domain (when all of r_1 , r_2 and r_{12} are large) but it is not accurate enough at finite distances. Similar calculations are reported by Pont and Shakeshaft [5, 23, 29]. They used screened coulomb (2SC) wave functions (for the outgoing electrons) which is supposed to be a better wave function (but not asymptotically exact). The results are much better.

Later Lucey *et al* [30] tried various initial state and final state wave functions, including the 3C wave function (none accurate enough), tested gauge dependence and found much discrepancies in the results.

In this work, we consider yet another high level computational scheme which is capable of yielding reliable cross sections. This is the Hyperspherical partial wave approach of one of the authors (Das [31, 32, 33, 34], Das *et al* [35]) which is very successful in representing the three-particle continuum wave function in the final channel very accurately.

Here we use a 20-term correlated Hylleraas type wave function of the form

$$\Phi_i(r_1, r_2) = \aleph e^{-\frac{k}{2}(r_1+r_2)} \sum_{n_1, n_2, n_3} C_{n_1 n_2 n_3} (r_1 + r_2)^{n_1} (r_1 - r_2)^{n_2} r_{12}^{n_3} \quad (3)$$

given by Hart and Herzberg [20] for the helium ground state and use the final channel wave function calculated in the hyperspherical partial wave approach as indicated below.

It may be noted here that our present approach and the HRM-SOW approach are similar in some respects, although ours is a fully quantal approach whereas the HRM-SOW approach is partly semi classical. From the recent calculations of Selles *et al* on HRM-SOW approach, it is clear that for unequal energy sharing kinematics one needs to consider the asymptotic range parameter R_∞ (considered below) to have values of several thousands a.u. for converged results, whereas for equal energy sharing cases only few hundreds suffice. So we restrict our present study to equal energy sharing cases only, which is much easier.

2. Hyperspherical Partial Wave Approach

In this section we outline the most salient features of this method. For the final state $\Psi_f^{(-)}$, which needs more accurate treatment, we use hyperspherical co-coordinates $R = \sqrt{r_1^2 + r_2^2}$, $\alpha = \text{atan}(r_2/r_1)$, $\hat{r}_1 = (\theta_1, \phi_1)$, $\hat{r}_2 = (\theta_2, \phi_2)$ and $\omega = (\alpha, \hat{r}_1, \hat{r}_2)$ and put $P = \sqrt{p_1^2 + p_2^2}$, $\alpha_0 = \text{atan}(p_2/p_1)$, $\hat{p}_1 = (\theta_{p_1}, \phi_{p_1})$, $\hat{p}_2 = (\theta_{p_2}, \phi_{p_2})$ and $\omega_0 = (\alpha_0, \hat{p}_1, \hat{p}_2)$, \vec{p}_1 , \vec{p}_2 being momenta of the two outgoing electrons of energies E_1 and E_2 and coordinates \vec{r}_1 , \vec{r}_2 . We expand $\Psi_f^{(-)}$ in hyperspherical harmonics (Das

[32], Lin [36]) which are functions of the above five angular variables and depend on the variables ℓ_1, ℓ_2, n, L, M (collectively called λ) which are respectively the angular momenta of the two electrons, the order of the Jacobi polynomial and the total angular momentum and its projection, in addition to the dependence on S , the total spin. It may be noted that L, S, π (the parity) are conserved here.

Thus we decompose the symmetrized wave function $\Psi_{fs}^{(-)}$ as

$$\Psi_{fs}^{(-)}(R, \omega) = \sqrt{\frac{2}{\pi}} \sum_{\lambda} \frac{F_{\lambda}^s(\rho)}{\rho^{\frac{5}{2}}} \phi_{\lambda}^s(\omega), \quad (4)$$

following the expansion of the symmetrized plane wave [20]

$$\begin{aligned} & [\exp(i\vec{p}_1 \cdot \vec{r}_1 + i\vec{p}_2 \cdot \vec{r}_2) + (-1)^s \exp(i\vec{p}_2 \cdot \vec{r}_1 + i\vec{p}_1 \cdot \vec{r}_2)] / (2\pi)^3 \\ &= \sqrt{\frac{2}{\pi}} \sum_{\lambda} i^{\lambda} \frac{j_{\lambda}^s(\rho)}{\rho^{\frac{3}{2}}} \phi_{\lambda}^{s*}(\omega_0) \phi_{\lambda}^s(\omega). \end{aligned} \quad (5)$$

Here $\lambda = \ell_1 + \ell_2 + 2n$ and $\rho = PR$.

The F_{λ}^s satisfy an infinite coupled set of equations

$$\left[\frac{d^2}{d\rho^2} + 1 - \frac{\nu_{\lambda}(\nu_{\lambda} + 1)}{\rho^2} \right] F_{\lambda}^s(\rho) + \sum_{\lambda'} \frac{2\alpha_{\lambda\lambda'}^s}{P\rho} F_{\lambda'}^s(\rho) = 0 \quad (6)$$

where

$$\alpha_{\lambda\lambda'}^s = -\langle \phi_{\lambda}^s | C | \phi_{\lambda'}^s \rangle, \quad (7)$$

$$C = -\frac{1}{\cos\alpha} - \frac{1}{\sin\alpha} + \frac{1}{|\hat{r}_1 \cos\alpha - \hat{r}_2 \sin\alpha|} \quad (8)$$

and $\nu_{\lambda} = \lambda + \frac{3}{2}$ (note that we use λ with two different meanings depending on the context). Here the radial waves with $L=1, S=0$ and $\pi = -1$ are relevant for the T-matrix calculations.

So here we fix $\mu = (L, S, \pi)$ with $L=1, S=0$ and $\pi = -1$, call it μ_0 and consider different $N = (\ell_1, \ell_2, n)$ and set $F_{\lambda}^s \equiv f_N^{\mu_0}$ in equation (6). Further we omit μ_0 from $f_N^{\mu_0}$ and write the relevant coupled set of equations (6) as

$$\left[\frac{d^2}{d\rho^2} + 1 - \frac{\nu_N(\nu_N + 1)}{\rho^2} \right] f_N^s + \sum_{N'} \frac{2\alpha_{NN'}^s}{P\rho} f_{N'}^s = 0. \quad (9)$$

For our numerical computations we truncate the set to some maximum value N_{mx} of N . These N_{mx} equations in N_{mx} variables are needed to be solved from origin to infinity. Actually we need construction of N_{mx} independent solutions which vanish at the origin. Now for convenience we divide the whole solution domain $(0, \infty)$ into three subdomains $(0, \Delta), (\Delta, R_{\infty})$ and (R_{∞}, ∞) , where Δ has the value of a few atomic units and R_{∞} is a point in the asymptotic domain. Best choices for these may be made by simple variations. Results do not depend significantly on these. But for converged results in some situations, values of R_{∞} , as in HRM-SOW calculation [9], are to be thousands of

atomic units. Next we proceed for solutions over subdomains. For (R_∞, ∞) we have simple analytic solutions [32]:

$$f_{snN}^s(\rho) = \sum_{\ell} \frac{a_{kN}^{(\ell)} \sin \theta_k}{\rho^\ell} + \frac{b_{kN}^{(\ell)} \cos \theta_k}{\rho^\ell} \quad (10)$$

$$f_{snN}^s(\rho) = \sum_{\ell} \frac{c_{kN}^{(\ell)} \sin \theta_k}{\rho^\ell} + \frac{d_{kN}^{(\ell)} \cos \theta_k}{\rho^\ell} \quad (11)$$

where $f_{snN}^{(k)}$ and $f_{csN}^{(k)}$ are the N-th element of the k-th solution vectors. Obviously these give $2N_{mx}$ independent solution vectors. The coefficients in these expressions are determined through recurrence relations (see Das [32]) in terms of $a_{kN}^{(0)} = a_{kN}$ and $b_{kN}^{(0)} = 0$, $c_{kN}^{(0)} = 0$, $d_{kN}^{(0)} = a_{kN}$, a_{kN} being the N-th element of the k-th eigen vector of the charge matrix $A = (\alpha_{NN'})$. Here we have $\theta_k = \rho + \alpha_k \ln 2\rho$, α_k being the k-th eigen value of A.

Solution over (Δ, R_∞) is also very simple. Because of the simple structure of equations (9) a Taylors expansion method works nicely. Earlier for the (e, 2e) problem, Das also adopted this approach [33, 34]. But the main difficulty lies in the construction of the solution vectors over $(0, \Delta)$. In those calculations on (e, 2e) problem Das used an approach as in R-matrix calculations [37]. But very often, this invites pseudo resonance type behaviour causing undesirable oscillations in the cross sections. Recently [35] for (e, 2e) problem, we applied the finite difference method (a five-point scheme) for solutions in the interval $(0, \Delta)$ and thereby get rid of undesirable oscillations. So we adopted here the same approach but with a seven-point scheme in place of the five-point scheme.

Thus for the solution in the interval $(0, \Delta)$ we recast equations (9) in terms of R instead of ρ , as

$$\left[\frac{d^2}{dR^2} + P^2 - \frac{\nu_N(\nu_N + 1)}{R^2} \right] f_N^s + \sum_{N'=1}^{N_{mx}} \frac{2 \alpha_{NN'}^s}{R} f_{N'}^s = 0, \quad (12)$$

and solve these equations as a two point boundary value problem by difference equation method. At $R = 0$, the solution vectors are set to zero while at $R = \Delta$ we assign to the k-th solution vector the k-th column of the unit matrix. The matrix for the corresponding difference equation is a sparse matrix and for its solution special methods are available. Here we use biconjugate gradient method [38]. We find that this method readily works and gives converged solutions.

Now for the difference equations we divide the interval $[0, \Delta]$ into m subintervals of length h with mesh points

$$0 = R_0 < R_1 < R_2 < \dots < R_k < \dots < R_{m-1} < R_m = \Delta$$

with $R_k = R_0 + kh$ and use the following seven-point difference formula:

$$\begin{aligned}
f_N''(R_k) &= \frac{1}{h^2} \left[\frac{1}{90} f_N(R_{k-3}) - \frac{3}{20} 16 f_N(R_{k-2}) \right. \\
&\quad + \frac{3}{2} f_N(R_{k-1}) - \frac{49}{18} f_N(R_k) + \frac{3}{2} f_N(R_{k+1}) - \frac{3}{20} 16 f_N(R_{k+2}) \\
&\quad \left. + \frac{1}{90} f_N(R_{k+3}) \right] + \left\{ \frac{69}{25200} h^6 f_N^{(viii)}(\xi_1) \right\}
\end{aligned} \tag{13}$$

for $k = 3, 4, \dots, m-4, m-3$, and for $k = 1, 2$ and $m-2, m-1$ the formulae

$$\begin{aligned}
f_N''(R_1) &= \frac{1}{h^2} \left[\frac{3}{8} f_N(R_0) + 6 f_N(R_1) - \frac{11}{2} h^2 f_N''(R_2) \right. \\
&\quad \left. - \frac{51}{4} f_N(R_3) - h^2 f_N''(R_3) + 6 f_N(R_4) + \frac{3}{8} f_N(R_4) \right] \\
&\quad + \left\{ -\frac{23}{10080} h^6 f^{(viii)}(\xi_2) \right\}.
\end{aligned} \tag{14}$$

$$\begin{aligned}
f_N''(R_2) &= \frac{1}{h^2} \left[\frac{3}{8} f_N(R_1) + 6 f_N(R_2) - \frac{11}{2} h^2 f_N''(R_3) - \frac{51}{4} f_N(R_3) \right. \\
&\quad \left. - h^2 f_N''(R_4) + 6 f_N(R_4) + \frac{3}{8} f_N(R_5) \right] \\
&\quad + \left\{ -\frac{23}{10080} h^6 f^{(viii)}(\xi_3) \right\}.
\end{aligned} \tag{15}$$

$$\begin{aligned}
f_N''(R_{m-2}) &= \frac{1}{h^2} \left[\frac{3}{8} f_N(R_{m-5}) + 6 f_N(R_{m-4}) - h^2 f_N''(R_{m-4}) - \frac{51}{4} f_N(R_{m-3}) \right. \\
&\quad \left. - \frac{11}{2} h^2 f_N''(R_{m-3}) + 6 f_N(R_{m-2}) + \frac{3}{8} f_N(R_{m-1}) \right] \\
&\quad + \left\{ -\frac{23}{10080} h^6 f^{(viii)}(\xi_4) \right\}.
\end{aligned} \tag{16}$$

and

$$\begin{aligned}
f_N''(R_{m-1}) &= \frac{1}{h^2} \left[\frac{3}{8} f_N(R_{m-4}) + 6 f_N(R_{m-3}) - h^2 f_N''(R_{m-3}) - \frac{51}{4} f_N(R_{m-2}) \right. \\
&\quad \left. - \frac{11}{2} h^2 f_N''(R_{m-2}) + 6 f_N(R_{m-1}) + \frac{3}{8} f_N(R_m) \right] \\
&\quad + \left\{ -\frac{23}{10080} h^6 f^{(viii)}(\xi_5) \right\}.
\end{aligned} \tag{17}$$

The quantities on the right hand sides within curly brackets represent the error terms. The corresponding difference equations are obtained by substituting these expressions the values of second order derivatives from the differential equation (12). For continuing these solutions in the domain (Δ, R_∞) we need first order derivatives $f'_N(R)$ at Δ . These are computed from the difference formula

$$\begin{aligned}
f'_N(R_m) &= \frac{1}{84h} [-f_N(R_{m-4}) + 24f_N(R_{m-2}) - 128f_N(R_{m-1}) + 105f_N(R_m)] \\
&\quad + \frac{2h}{7} f_N''(R_m) + \left\{ -\frac{4h^4}{105} f_N^{(v)}(\xi) \right\}
\end{aligned} \tag{18}$$

Here too, the quantity within curly brackets represents the error term. The solutions thus obtained in $(0, \Delta)$ are then continued over (Δ, R_∞) by Taylor's expansion method,

as stated earlier, with stabilization after suitable steps [39]. The N_{mx} independent solution vectors so obtained, are put together to get the solution matrix f_0 . The solution matrices f_{sn} and f_{cs} are similarly obtained, whose N-kth element are respectively $f_{sn}^{(k)}$ and $f_{csN}^{(k)}$, given by (10) and (11) respectively.

Next we introduce the K-matrix through the relation

$$f_0 \cdot B = f_{sn} + f_{cs} \cdot K \quad (19)$$

where B is an unknown constant matrix. The K-matrix is determined from matching values and first order derivatives at R_∞ , where all of f_0 , f_{sn} and f_{cs} are valid. (It may be noted here that there is a slight departure in our definition of K-matrix from the usual practice. However, it is symmetric as it should be).

Finally the physical scattering state with appropriate boundary conditions is taken as

$$\mathbf{f}_{\text{ph}} = f_0 \cdot \mathbf{g} \quad (20)$$

and also we have

$$\begin{aligned} \mathbf{f}_{\text{ph}} &= (f_{sn} + f_{cs} \cdot K) \cdot \mathbf{c} \\ &= f_{sn} \cdot \mathbf{c} + f_{cs} \cdot \mathbf{d} \end{aligned} \quad (21)$$

with

$$\mathbf{d} = K \cdot \mathbf{c}. \quad (22)$$

Thus the physical state is completely determined once the vector \mathbf{c} is determined. Now \mathbf{c} is determined from the consideration that $\Psi_{fs}^{(-)}$ is asymptotically a (distorted) plane wave (representing the two outgoing electrons) plus incoming waves only. So the coefficients of the outgoing wave $\exp(i\rho)$ of both $\Psi_{fs}^{(-)}$ and the symmetrized plane wave (equation (5)) must be the same (except for the distorting term $\exp(i\alpha_k \ln 2\rho)$). This requires

$$\mathbf{c} = [I + iK]^{-1} \mathbf{P} \quad (23)$$

where

$$\mathbf{P} = -2e^{i\frac{\pi}{4}} X^{-1} \Phi^{\text{s}*}(\omega_0), \quad (24)$$

and X is the matrix comprising of the columns of eigen vectors of the charge matrix A and $\Phi^{\text{s}*}$ is given by

$$\Phi^{\text{s}*}(\omega_0) = \begin{pmatrix} \phi_1^{\text{s}*}(\omega_0) \\ \vdots \\ \phi_{N_{mx}}^{\text{s}*}(\omega_0) \end{pmatrix}. \quad (25)$$

Finally the DPI triple differential cross section is given by

$$\frac{d^3\sigma}{d\Omega_1 d\Omega_2 dE_1} = \frac{2\pi^2 \alpha p_1 p_2}{\omega_i} |T_{fi}|^2, \quad (26)$$

after the inclusion of μ_0 -part of $\Psi_{fs}^{(-)}$ in T_{fi} .

3. Results

In our present calculation we have applied the above hyperspherical partial wave approach both in length and velocity gauges. Here we consider equal-energy-sharing case, since then the computational problem becomes little simple. For this calculation we have chosen $\Delta = 5$ a.u., $R_\infty = 300$ a.u., $h = 0.05$ a.u. upto Δ and 0.1 a.u. beyond Δ . We have included 90 coupled channels with n upto 9 and (l_1, l_2) combinations nearly as in ECS calculation [40] for electron - hydrogen ionization collision. We have chosen the case of ionization at 20 eV excess energy as it has been widely considered and for which there are interesting experimental results [10]. For the present calculations with 90 channels and $R_\infty = 300$ a.u., our single differential cross section (SDCS) is little above the desired value of about 0.93 Kb/eV at $E/2$ (E being the excess photon energy). So we normalized our TDCS by scaling with a factor 0.8 (which is also the factor we use to scale our SDCS to get the desired value of 0.93 Kb/eV at $E/2$) both in the length and in the velocity gauges. The TDCS results thus obtained are presented in figure 1. Here we compare our results with the experimental results of Bräuning *et al* [10] and with the theoretical results of the CCC calculation only [10, 41], since the overall agreement of the CCC results are known to be somewhat better compared to the results of other calculations like TDCC, HRM-SOW etc. In all the cases the agreement between the velocity and length gauge calculations is excellent everywhere. We also did calculations in the acceleration gauge and these are indistinguishable from those of the velocity gauge. Agreement with the experimental results and with the CCC results are also generally good except for some spurious peaks at $\theta_{p_1} = 0^\circ$. The CCC results appear a little better compared to ours.

For unequal energy sharing our approach also works and we have reasonably good results. But for fully converged results, we have to consider larger l values for R_∞ . So we wish to report such results in future when our study is completed.

4. Conclusions

The present calculation, reported here, has only approximately converged. The results we have obtained, go to show that the hyperspherical three-particle scattering state wave function, used in the present calculation, must be reasonably accurate from small distances to the asymptotic region, since the results in all the three gauges are practically identical. In contrast, the 3C or other similar wave functions, which are not accurate at finite distances, show strong gauge dependence [30]. We also mention that the present calculation is free from any genuine difficulty and does not show any weakness worth mentioning. The present approach may easily be applied to DPI with varied types of polarization of the incident photons. With judicious choice of the parameter R_∞ and possibly with the availability of better computational facilities, the method may be applied from very low energy to high energy cases. At this point if we recall the capability of the hyperspherical partial wave approach in representing electron-hydrogen-atom

ionization collisions [33, 34, 35] at low energies (and also consider situations of very low energy cases, with excess energy 1 eV and below for which we had to take R_∞ about 4000 - 5000 a.u. and get reliable results for ionization cross sections [42]), consider the present success, then we may expect the hyperspherical partial wave theory to have a very good prospect.

Acknowledgments

We are grateful to H. Bräuning for providing us with the experimental results and to Igor Bray and Anatoly Kheifets for providing us with the CCC results in electronic form. KC acknowledges support from the UGC in the form of a Minor Research Project F.PSW-035/02(ERO). SP is grateful to CSIR for providing a research fellowship.

References

- [1] Bizau J M and Wuillemier F J 1995 J. Electron Spectrosc. Relat. Phenom. **71** 205.
- [2] Dörner R *et al* 1996 Phys. Rev. Lett **76** 2654.
- [3] Whelitz R *et al* 1997 J. Phys. B: At. Mol. Opt. Phys. **30** L51.
- [4] Samson J A R, Stolte W C, He Z X, Cutler J N, Lu Y, Bartlett R J 1998 Phys. Rev. A **57** 1906.
- [5] Pont M and Shakeshaft R 1995 J. Phys. B: At. Mol. Opt. Phys. **28** L571.
- [6] Kheifets A K and Bray I 1998 Phys. Rev. **A58** 4501.
- [7] Colgan J, Pindzola M S and Robichaux F 2001 J. Phys. B: At. Mol. Opt. Phys. **34** L457.
- [8] Malegat L, Selles P and Kazansky A K 2000 Phys. Rev. Lett. **85** 4450.
- [9] Selles P, Malegat L and Kazansky A K 2002 Phys. Rev. **A65** 032711.
- [10] Bräuning H, Dörner R, Cocke C L, Prior M H, Krässig B, Kheifets A S, Bray I, Bräuning-Demian A, Carnes K, Dreuil S, Mergel V, Richard P, Ulrich J and Schmidt-Böcking H 1998 J. Phys. B: At. Mol. Opt. Phys. **31** 5149.
- [11] Kheifets A S and Bray I 1998 J. Phys. B: At. Mol. Opt. Phys. **31** L447.
- [12] Kheifets A S and Bray I 1998 Phys. Rev. Lett. **81** 4588.
- [13] Kheifets A S and Bray I 2000 Phys. Rev. A **62** 065402.
- [14] Cvejanović S *et al* 2000 J. Phys. B: At. Mol. Opt. Phys. **33** 265.
- [15] Bolognesi P *et al* 2001 J. Phys. B: At. Mol. Opt. Phys. **34** 3195.
- [16] Dawson C *et al* 2001 J. Phys. B: At. Mol. Opt. Phys. **34** L525.
- [17] Briggs J S and Schmidt V 2000 J. Phys. B: At. Mol. Opt. Phys. **33** R1-R48.
- [18] Maulbetsch F and Briggs J S 1993 J. Phys. B: At. Mol. Opt. Phys. **26** 1679.
- [19] Chandrashekar S and Herzberg G 1955 Phys. Rev. **98** 1050.
- [20] Hart J F and Herzberg G 1957 Phys. Rev. **106** 79.
- [21] Pekeris C L 1958 Phys. Rev. **112** 1649.
- [22] Brauner M, Briggs J S and Klar H 1989 J. Phys. B: At. Mol. Opt. Phys. **22** 2265.
- [23] Pont M and Shakeshaft R 1995 Phys. Rev. A **51** R2676.
- [24] Huetz A, Selles P, Waymel P and Mageau J 1991 J. Phys. B: At. Mol. Opt. Phys. **24** 1917.
- [25] Achler M, Mergel V, Spielberger L, Dörner R, Azuma Y and Schmidt-Böcking H 2001 J. Phys. B: At. Mol. Opt. Phys. **34** 965.
- [26] Faegin J M 1995 J. Phys. B: At. Mol. Opt. Phys. **28** 1495.
- [27] Faegin J M 1996 J. Phys. B: At. Mol. Opt. Phys. **29** 1551.
- [28] Maulbetsch F, Briggs J S and Shakeshaft R 1995 J. Phys. B: At. Mol. Opt. Phys. **28** L341.
- [29] Pont M, Shakeshaft R, Maulbetsch F and Briggs J S 1996 Phys. Rev. A **53** 3671.
- [30] Lucy S P, Rasch J, Whelan C T and Walters H R H 1998 J. Phys. B: At. Mol. Opt. Phys. **31** 1237.
- [31] Das J N 1994 Aust. J. Phys. **47** 743.
- [32] Das J N 1998 Pramana-J. Phys. **50** 53.
- [33] Das J N 2001 Phys. Rev. A **64** 054703.
- [34] Das J N 2002 J. Phys. B: At. Mol. Opt. Phys. **35** 1165.
- [35] Das J N, Paul S and Chakrabarti K 2003 Phys. Rev. A(to be published).
- [36] Lin C D 1974 Phys. Rev. A **10** 1986.
- [37] Burke P G and Robb W D 1975 Adv. Atom. Mol. Phys. **11** 143.
- [38] Fletcher R 1975 *Numerical Analysis Dundee*, Lecture notes in Mathematics, Vol. 506, eds. A. Dold and B. Eckmann, Springer Verlag, Berlin, pp 73-89.
- [39] Choi B H and Tang K T 1975 J. Chem. Phys. **63** 1775.
- [40] Baertschy M, Rescigno T N, Isaacs W A, Li X and McCurdy C W 2001 Phys. Rev. A **63** 022712.
- [41] Kheifets A S 2003 Private communication.
- [42] Das J N, Paul S and Chakrabarti K 2003 J. Phys. B: At. Mol. Opt. Phys. (submitted)

Figure Captions

Figure 1. Triple differential cross sections for photo double ionization of the helium atom for equal energy sharing geometry for 20 eV excess energy and for a) $\theta_{p_1} = 0^\circ$, b) $\theta_{p_1} = 30^\circ$, c) $\theta_{p_1} = 60^\circ$, d) $\theta_{p_1} = 90^\circ$, θ_{p_1} being measured from the photon polarization direction. Theory : continuous curve, present calculation in velocity gauge; dashed curve present calculation in length gauge; dotted curve, CCC calculation [10]; Experiment : absolute measured values of Bräuning *et al*[10].

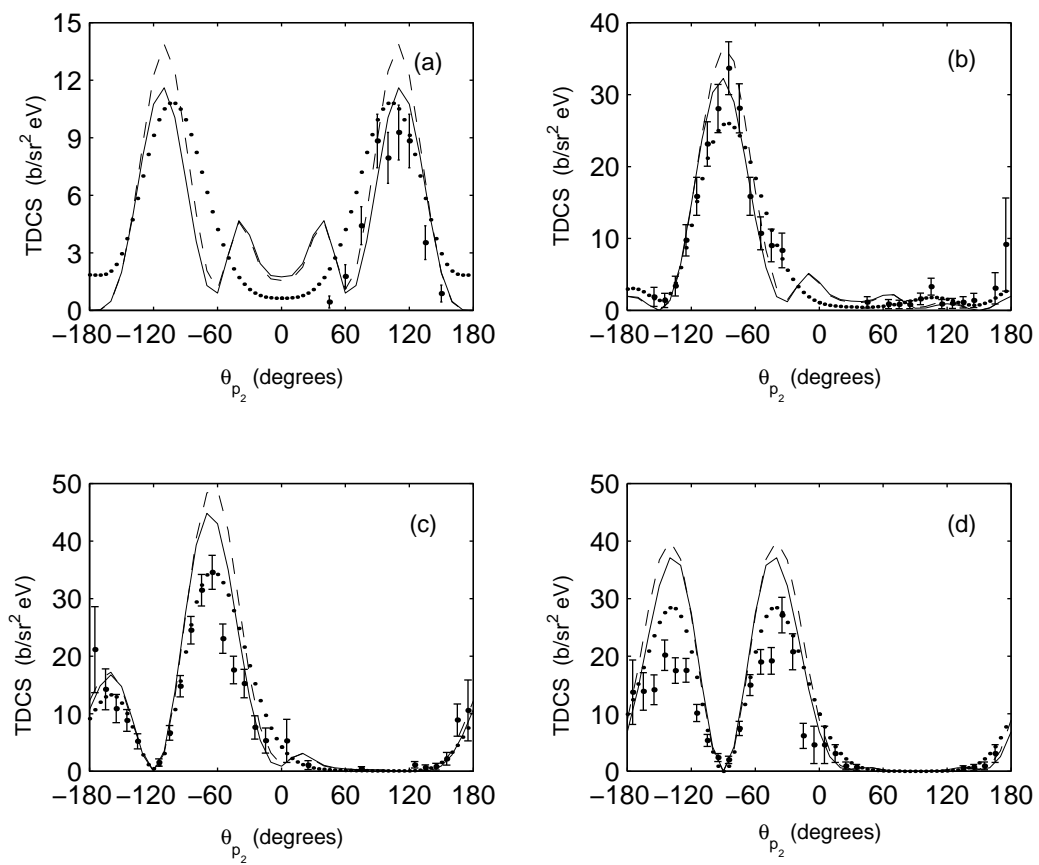


Figure 1